Electronic Supplementary Material (ESI) for New Journal of Chemistry.

Electronic Supplementary Information for "*Spin crossover in Hofmann-like coordination polymers. Effect of the axial ligand substituent and its position*" by

Y. Avila, O. Pérez, L. Sánchez, M. C. Vázquez, R. Mojica, M. González, M. Ávila, J. Rodríguez-Hernández, E. Reguera

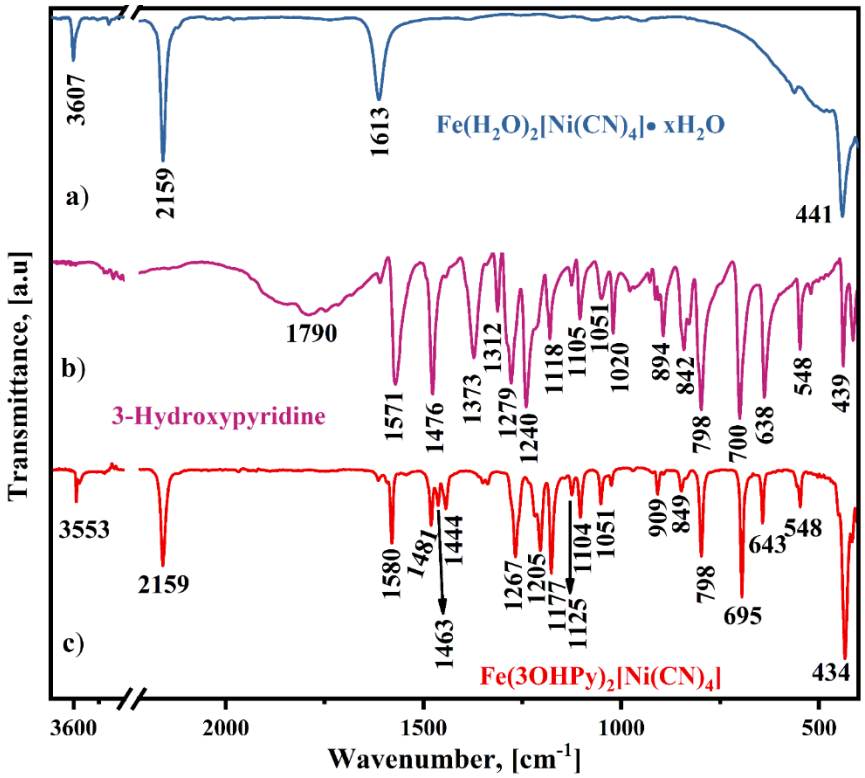

Figure S1. IR spectra for 2D ferrous tetracyanonickellate, 3-hydroxypyridine (3OHPy), and the solid obtained using the organic ligand as a pillar between adjacent layers, $Fe(3OHPy)_2[Ni(CN)_4]$.

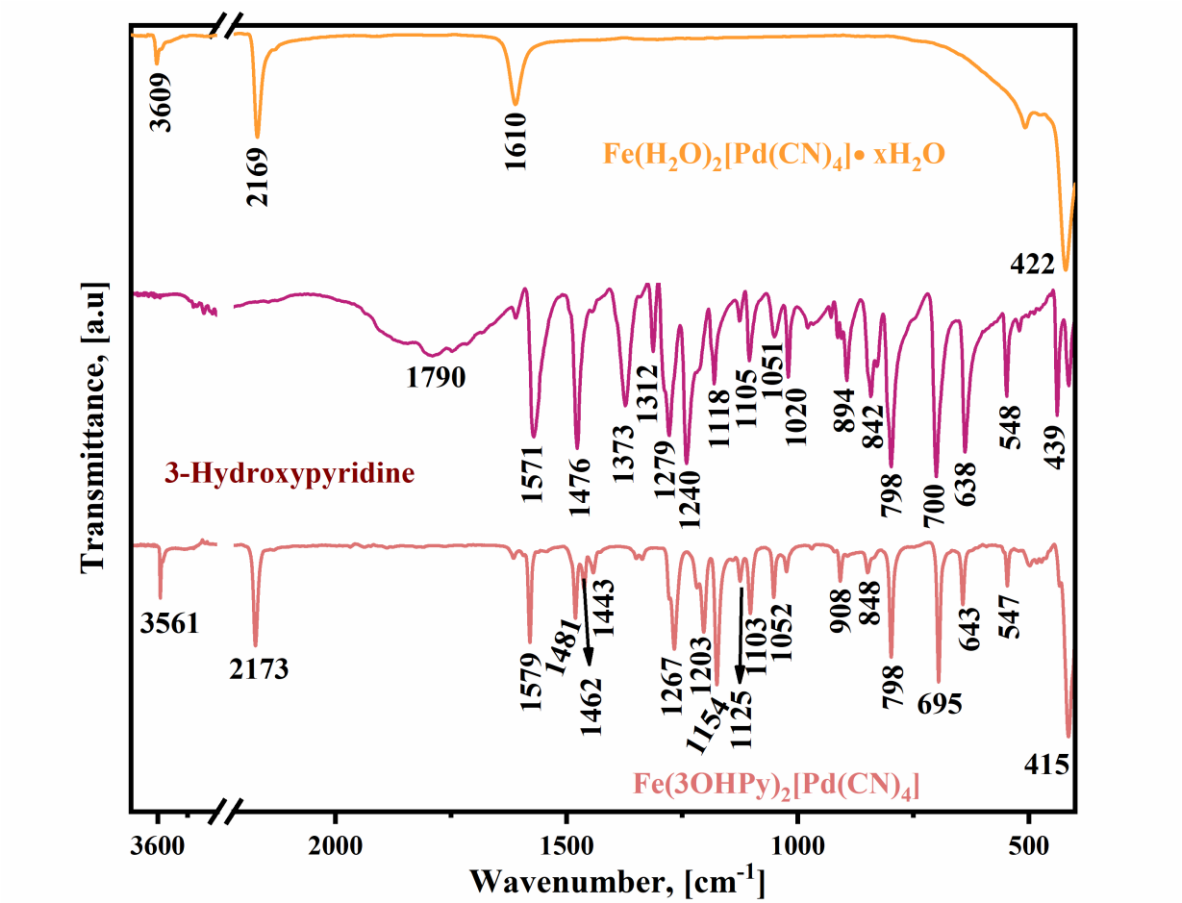

Figure S2. IR spectra for ferrous tetracyanopalladate, 3-hydroxypyridine, and the solid formed by the precipitation reaction of potassium tetracyanopalladate, ferrous ammonium sulfate, and the organic ligand.

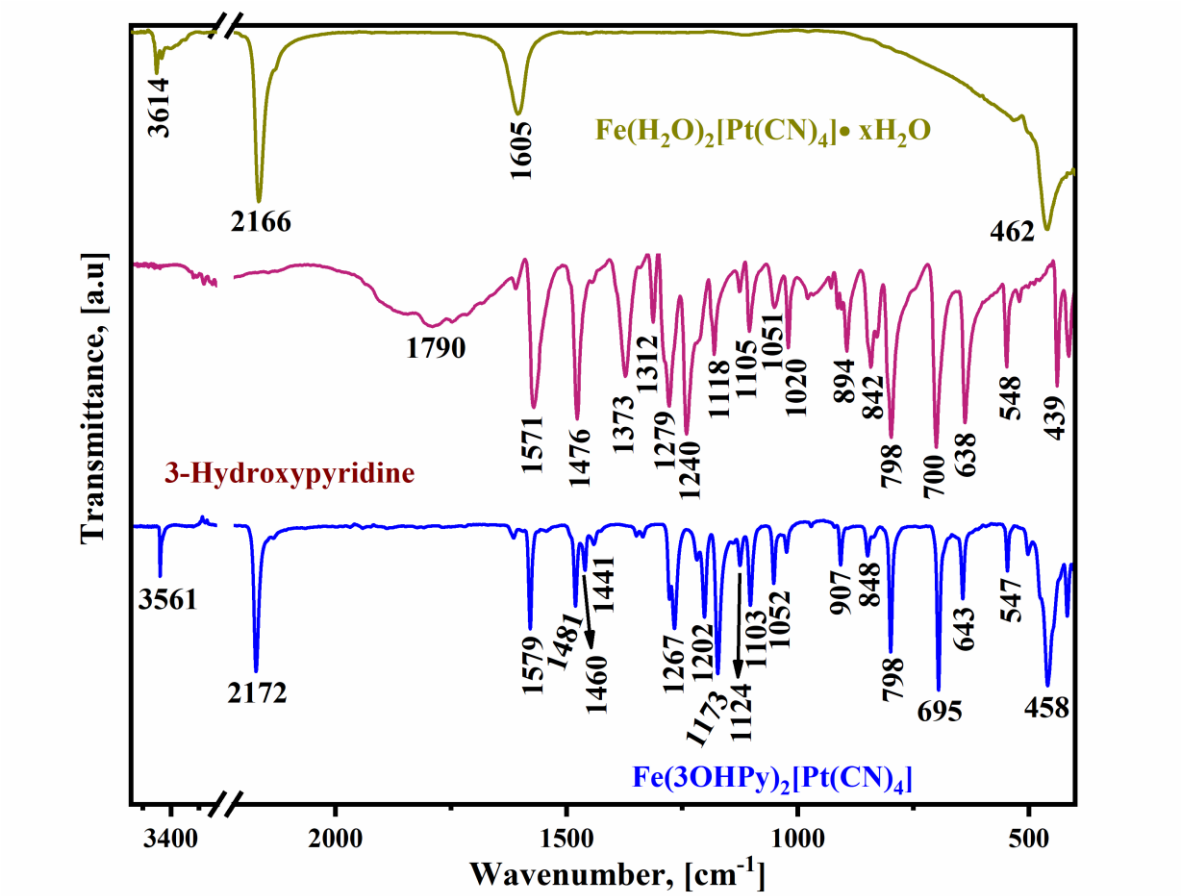

Figure S3. IR spectra for ferrous tetracyanoplatinate, 3-hydroxypyridine, and the solid formed by the precipitation reaction of potassium tetracyanoplatinate, ferrous ammonium sulfate, and the organic ligand.

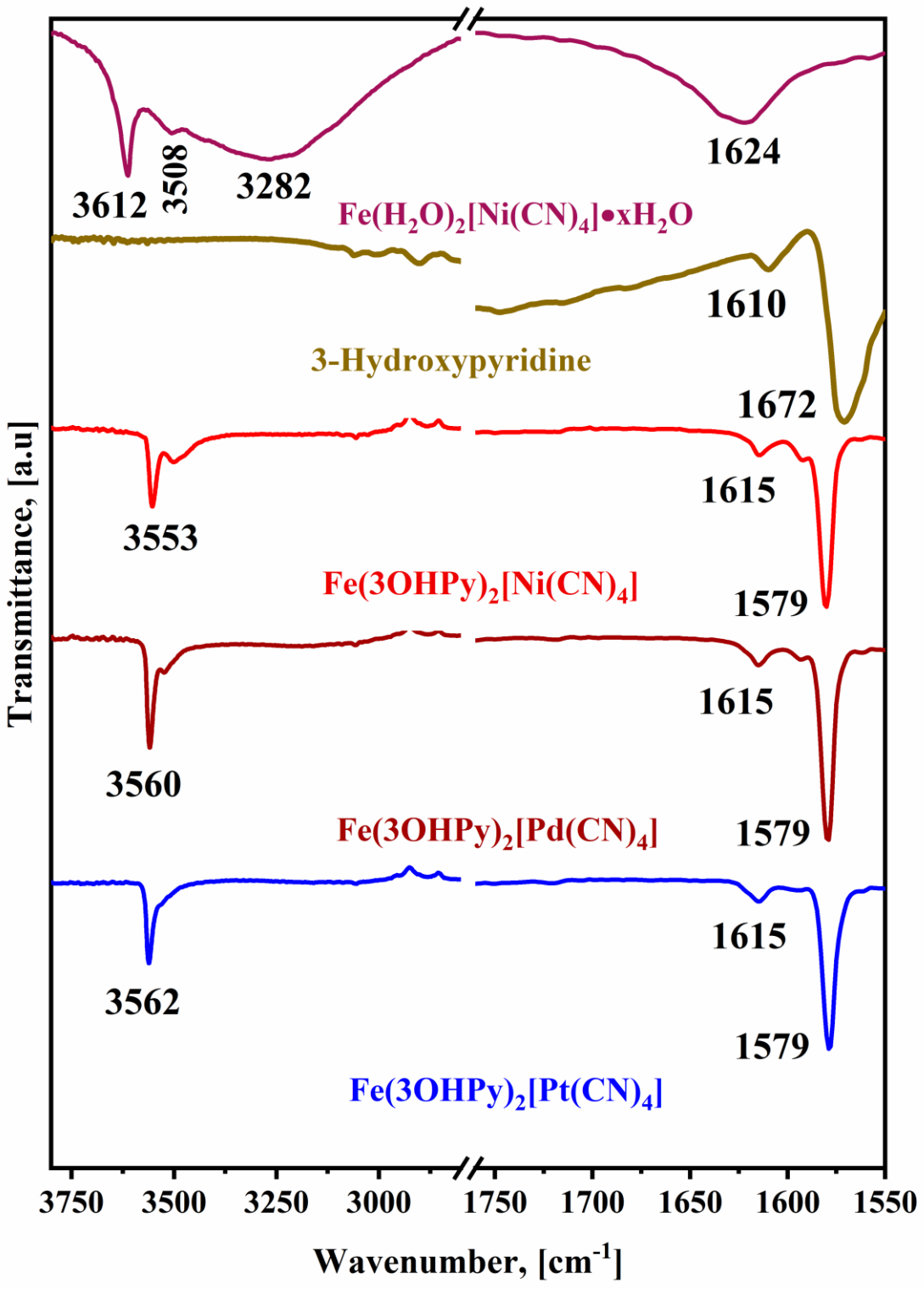
3612
3508
3282
1624
Fe(H2O)2[Ni(CN)4]•xH2O
1610
3-Hydroxypyridine
1672
1615
3553
Fe(3OHPy)2[Ni(CN)4]
1579
1615
3560
Fe(3OHPy)2[Pd(CN)4]
1579
1615
3562
1579
Fe(3OHPy)2[Pt(CN)4]
Transmittance, [a.u]
3750
3500
3250
3000
1750
1700
1650
1600
1550
Wavenumber, [cm-1]

Figure S4. ν(OH) and δ(HOH) spectral region of $Fe(H_2O)_2[Ni(CN)_4]\cdot nH_2O$, 3-hydroxypyridine; and the $Fe(3OHPy)_2[M(CN)_4]$ series with M = Ni, Pd, Pt. The ν(OH) and δ(HOH) absorption bands of $Fe(H_2O)_2[Ni(CN)_4]\cdot 4H_2O$ are absent in the formed coordination polymers. In this hydrated, the presence of the coordinated water molecules is probed by the appearance of two narrow ν(OH) bands at 3612 and 3508 cm^{-1}. The broad band at 3282 cm^{-1} corresponds to hydrogen-bonded water molecules. In the δ(HOH) spectral region, these two types of water molecules produce an intense unresolved doublet at 1624 cm^{-1}. That set of ν(OH) and δ(HOH) absorption bands are absent in the formed coordination polymers (Fig. S4, ESI). During the organic ligand coordination to the iron atom, the molecule's vibrational spectrum suffers significant changes, among them, the narrowing and shift to higher frequency values of their absorption bands (Fig. S1 to S3). The narrow absorption observed at 1615 cm^{-1} was ascribed to these effects, and not the δ(HOH) vibration of water molecules. The band observed at 3560 cm^{-1} was tentatively ascribed to a combination band of the organic ligand. The presence of a small fraction of water molecules in the formed hybrid solid cannot be discarded. These hybrid materials are obtained by a precipitation reaction using water as a solvent.

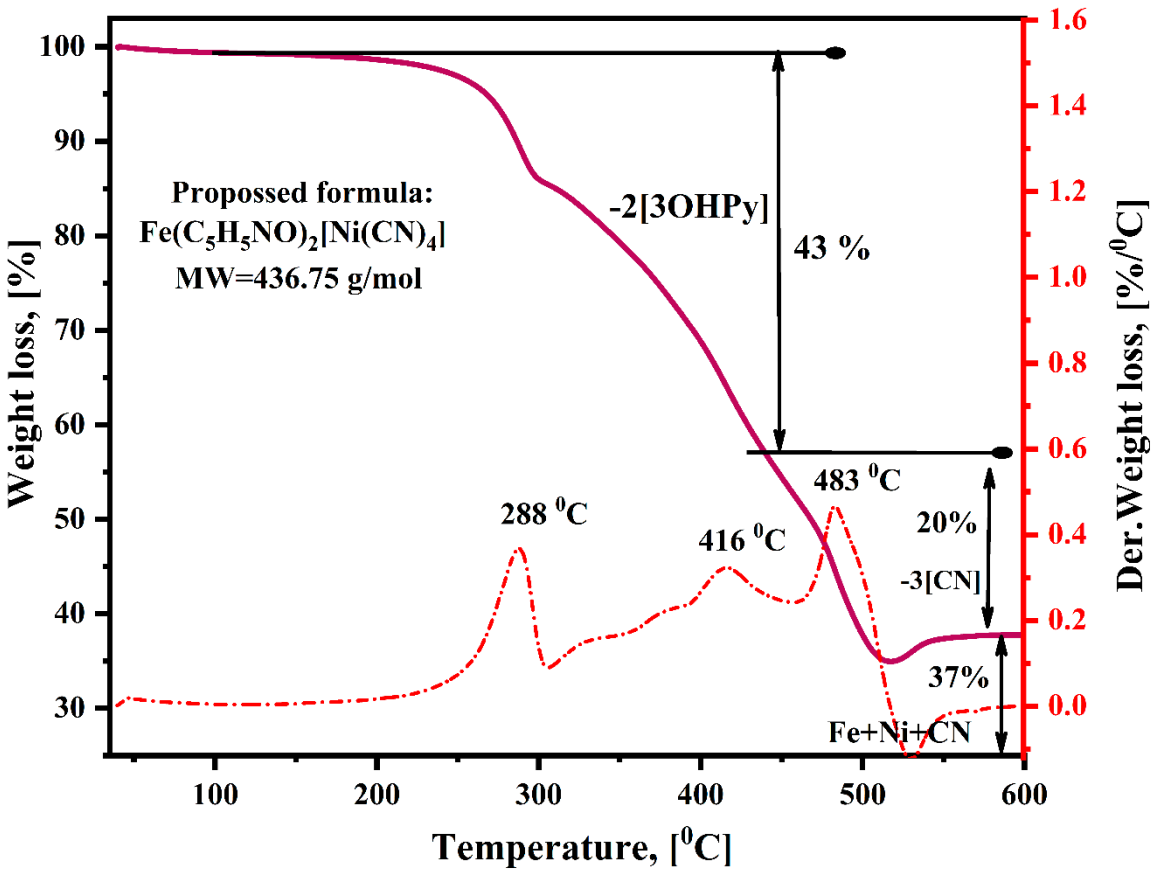

Figure S5. TG curve for the solid formed from the precipitation reaction of aqueous solutions of $K_2[Ni(CN)_4]$, Mohr salt, and the organic ligand (3OHPy).

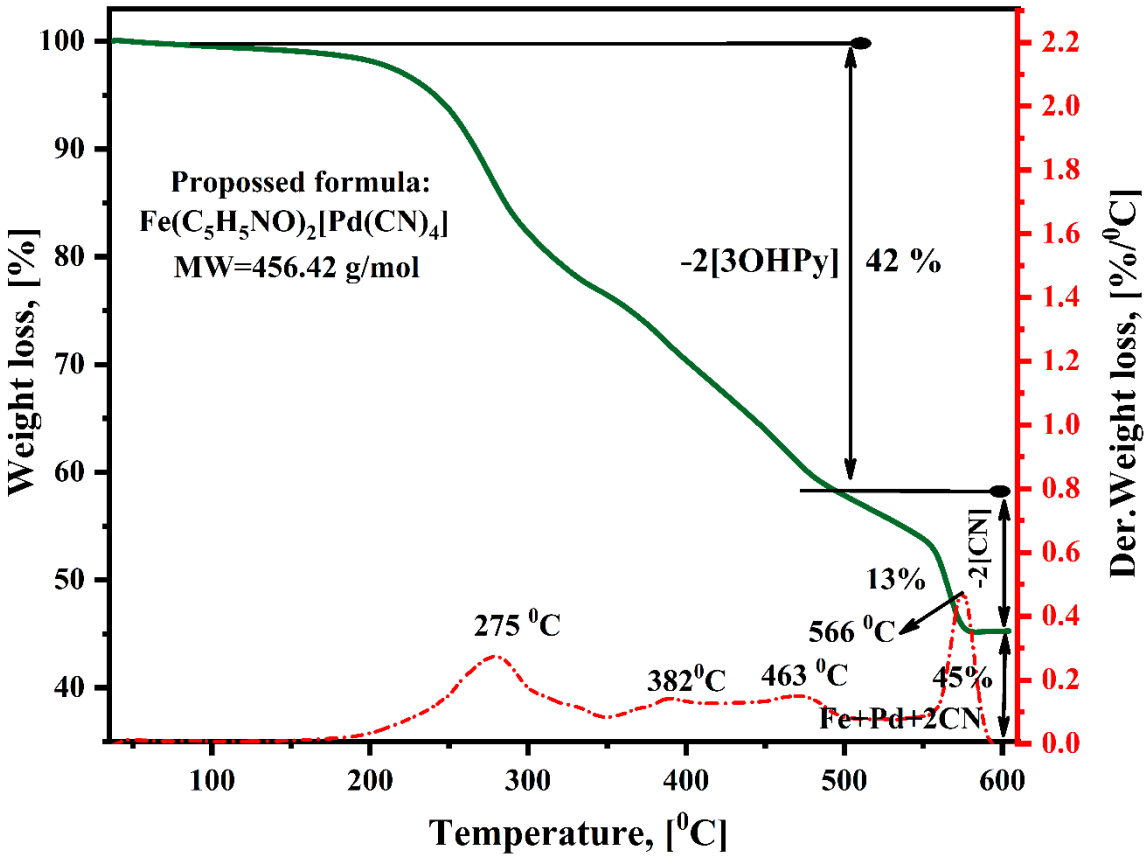

Figure S6. TG curve for the solid formed from the precipitation reaction of aqueous solutions of $K_2[Pd(CN)_4]$, Mohr salt, and the organic ligand (3OHPy).

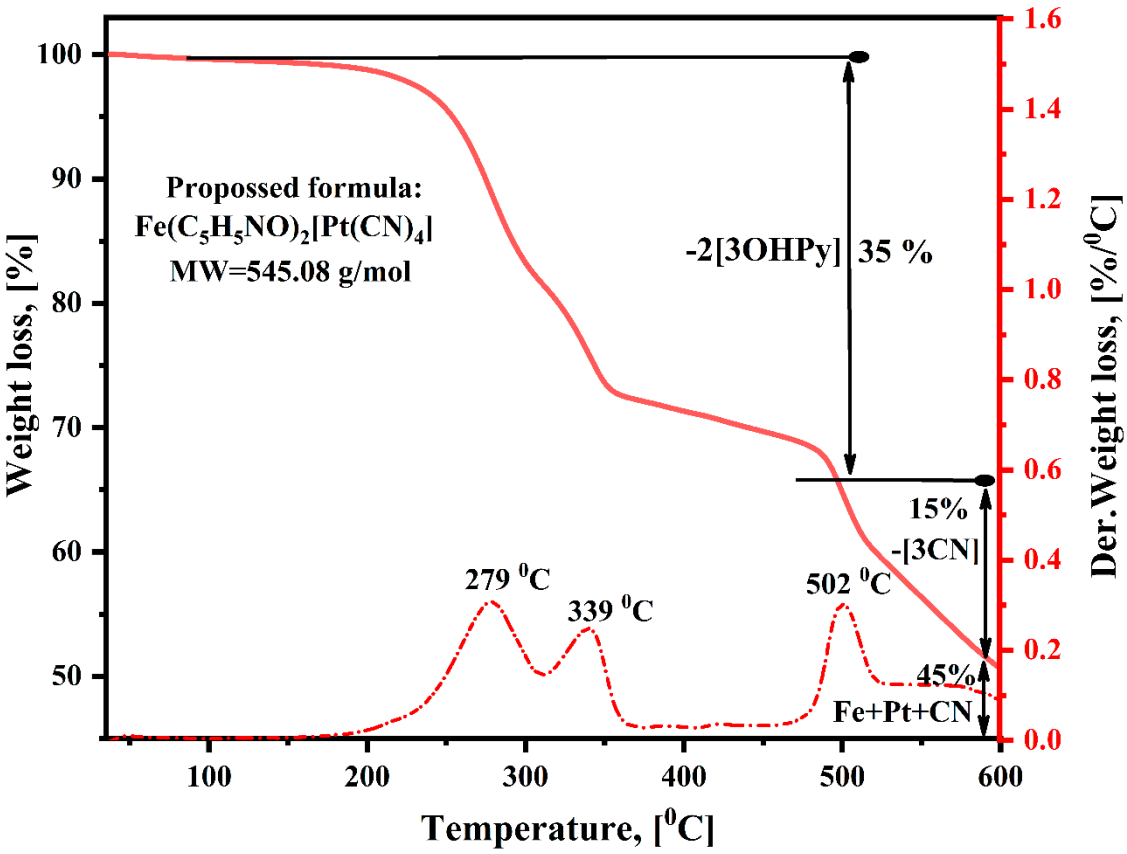

Figure S7. TG curve for the solid formed from the precipitation reaction of aqueous solutions of $K_2[Pt(CN)_4]$, Mohr salt, and the organic ligand (3OHPy).

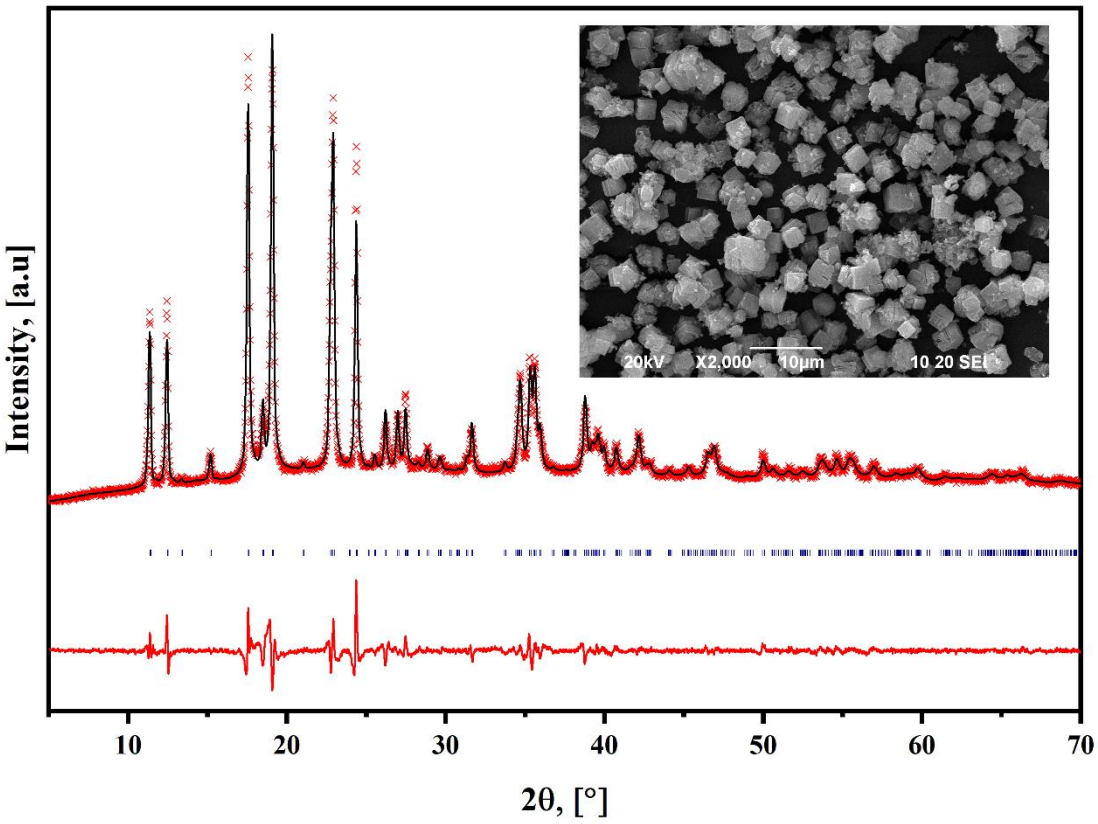

Figure S8. Experimental and fitted XRD powder patterns, and their difference for $Fe(3OHPy)_2[Ni(CN)_4]$. Inset: Morphology for the crystallites of the obtained solid.

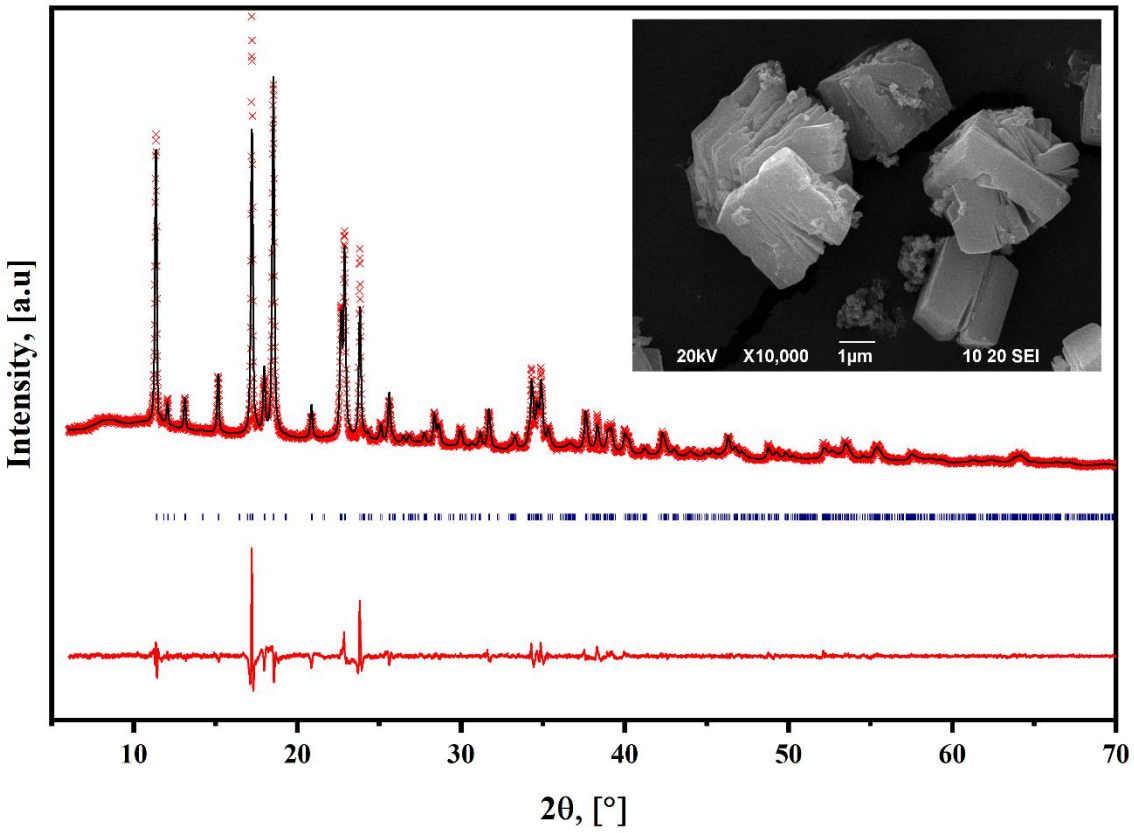

Figure S9. Experimental and fitted XRD powder patterns, and their difference for $Fe(3OHPy)_2[Pd(CN)_4]$. Inset: Morphology for the crystallites of the obtained solid.

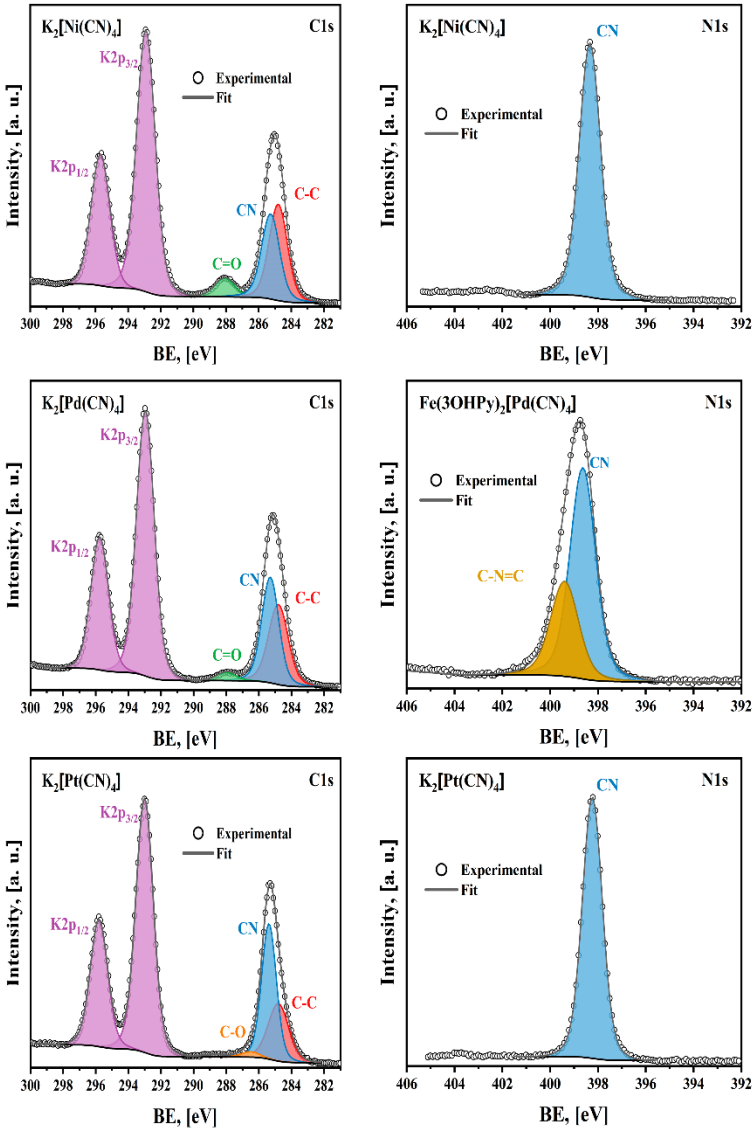

Figure S10. Experimental and fitted C1s and N1s spectral regions for the $K_2[Ni(CN)_4]$, $K_2[Pd(CN)_4]$and $K_2[Pt(CN)_4]$ salts.

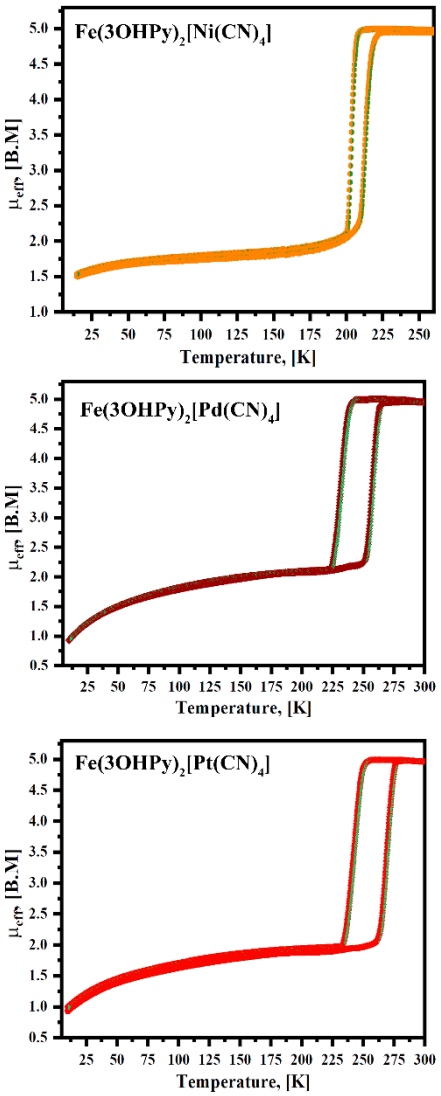

Figure S11. μ_{eff} versus temperature curves for the entire temperature region explored through the magnetic measurements. Below 50 K a definite antiferromagnetic interaction is observed, ascribed to the fraction of iron atoms that remain in the HS state due to the mentioned kinetic effects.

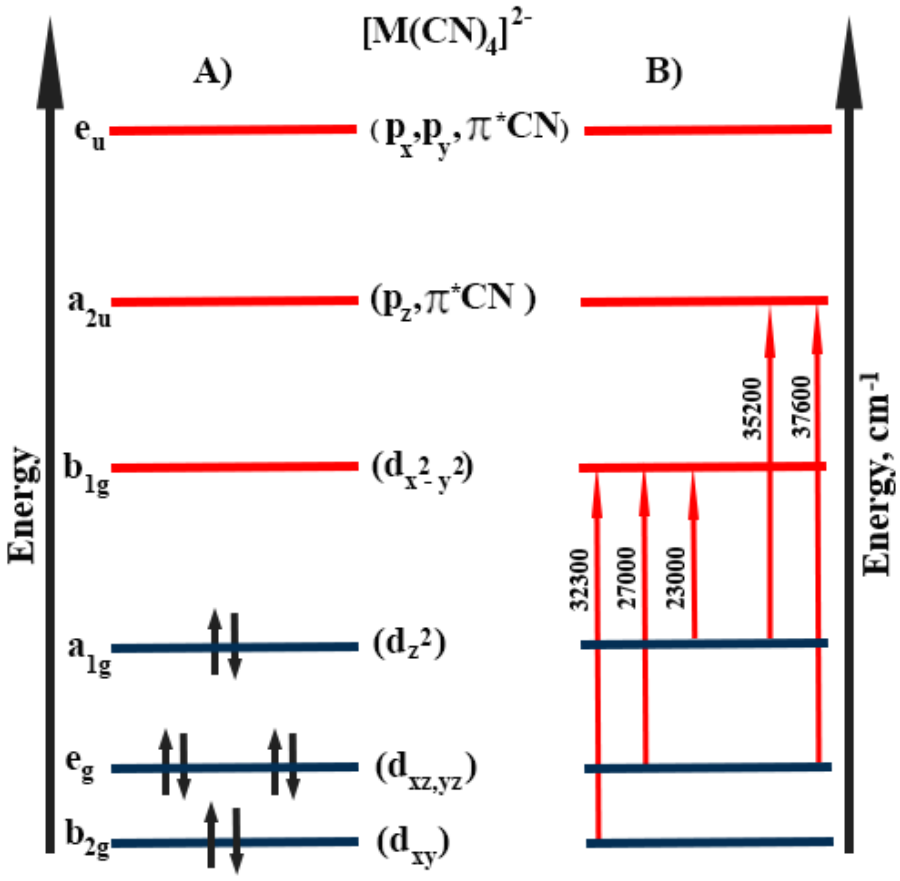

Figure S12. Energy diagram (d-d transitions) for the $[M(CN)_4]^{2-}$ ion in the absence of relativistic effects. These d-d transitions in the 37600-23000 cm^{-1} range correspond to absorption bands in the UV spectral region, from 266 to 435 nm.

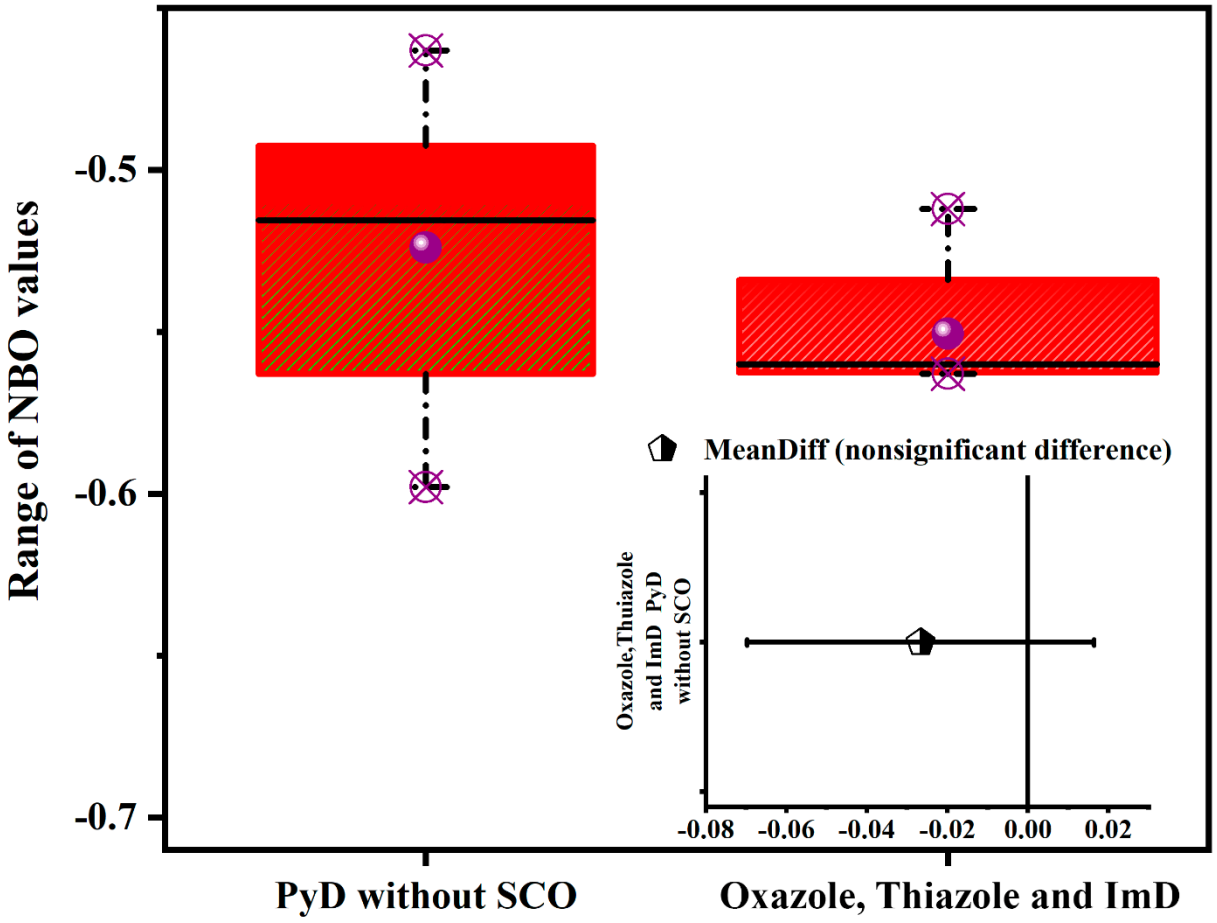

Figure S13. ANOVA test for the electron density (from NBO calculations) at the N-pyridinic atom in pyridine derivatives (PyD) forming Hofmann-like coordination polymers without SCO and oxazole, thiazole, and imidazole and its derivatives (ImD), including oxazole and thiazole, which form analogs solids.

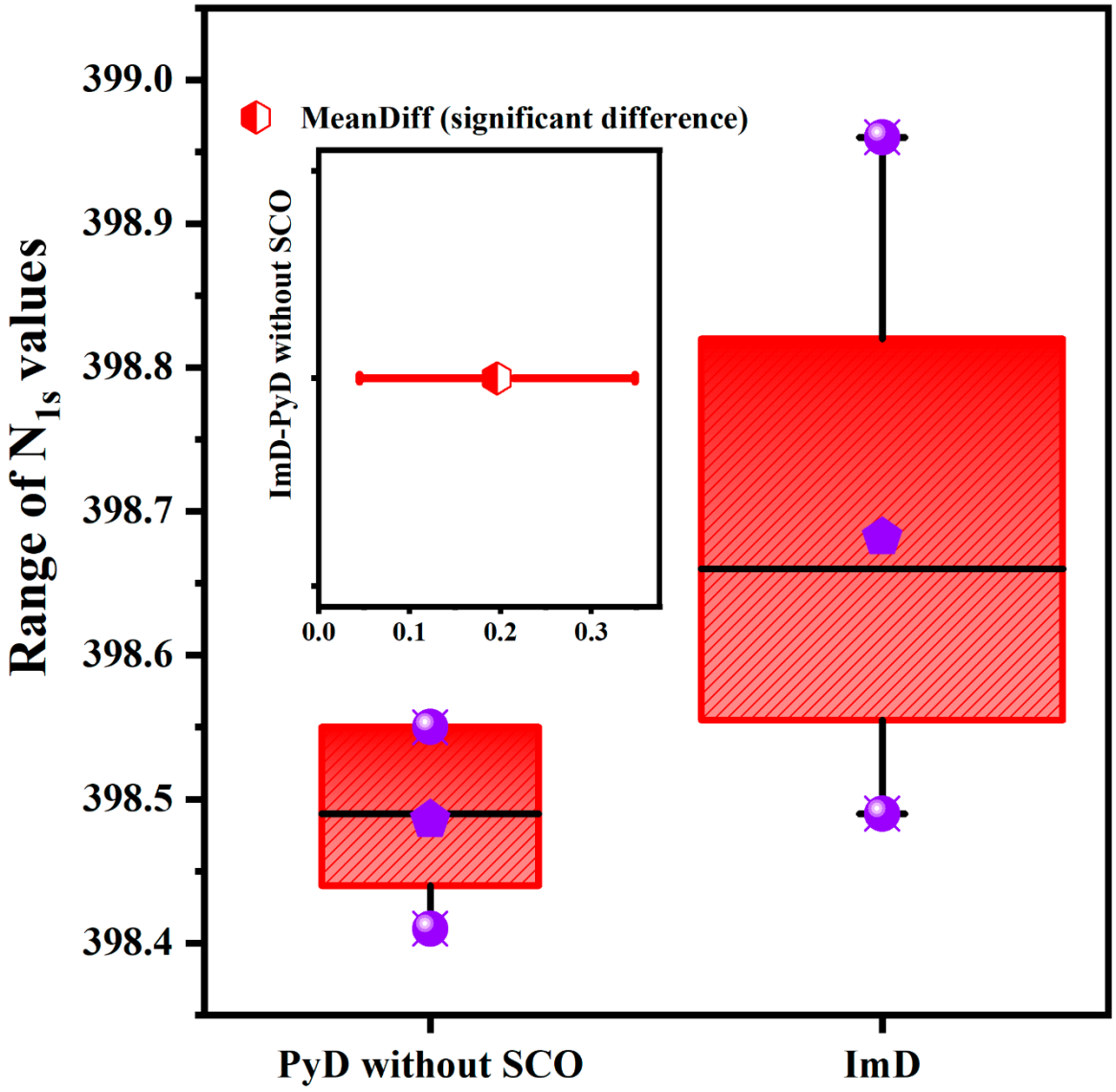

Figure S14. ANOVA analysis for the N1s values of $Fe(L)_2[M(CN)_4]$, L= pyridine derivatives (PyD) without SCO and $Fe(ImD)_2[Ni(CN)_4]$ Hofmann-like coordination polymers, ImD: imidazole and its derivatives, including thiazole and oxazole.

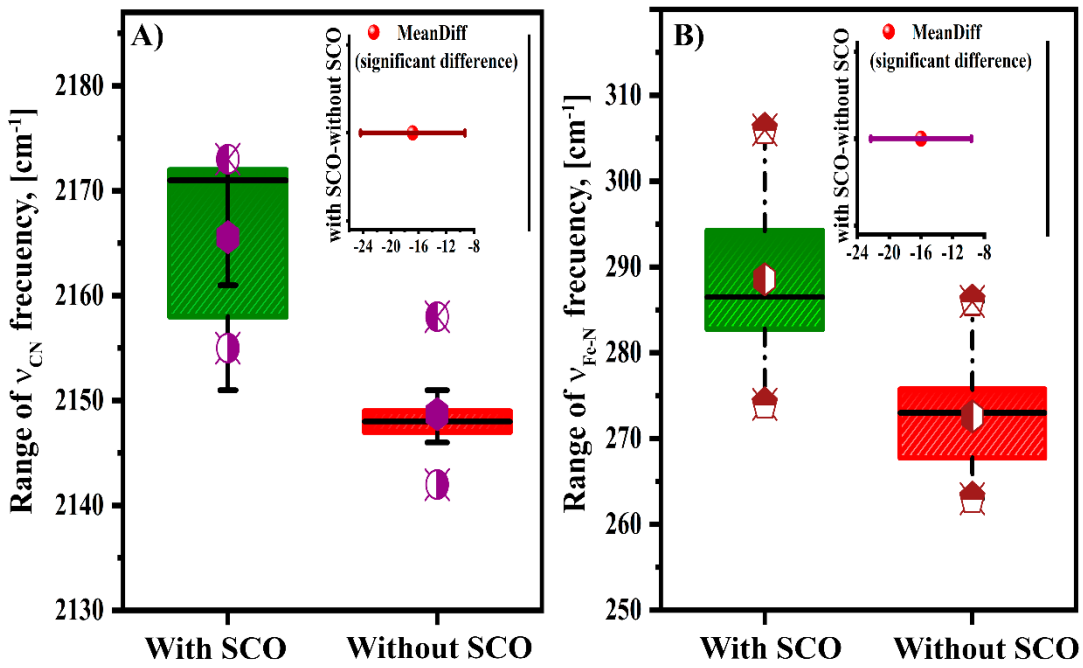

Figure S15. ANOVA analysis for the frequency values of the ν(CN) (Left) and ν(Fe-N_L) (right) stretching vibrations in Hofmann-like solids with and without SCO on the sample cooling. The average frequency values and their dispersion for these two vibrations are significantly different in the considered two populations of samples.

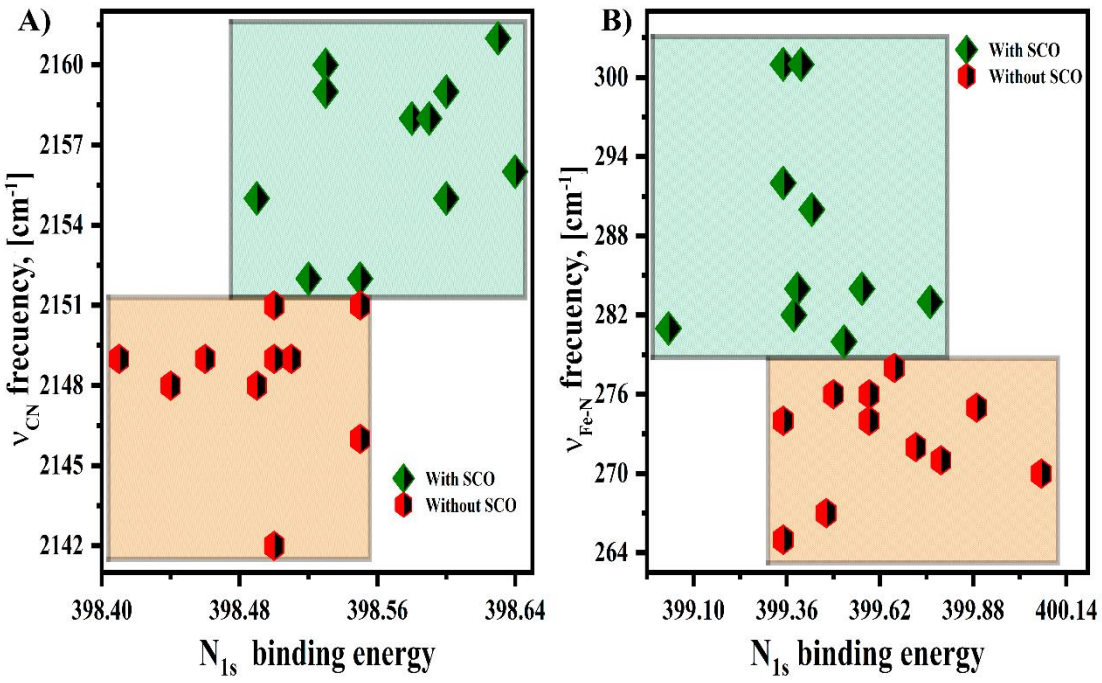

Figure S16. A) Plot of ν(CN) frequency versus N1s BE for the CN ligand. B) Plot of ν(Fe-N_L) frequency versus N1s BE for the N-pyridinic atom in the organic ligand. These plots correspond to Hofmann-like solids, $Fe(L)_2[M(CN)_4]$, with and without SCO.

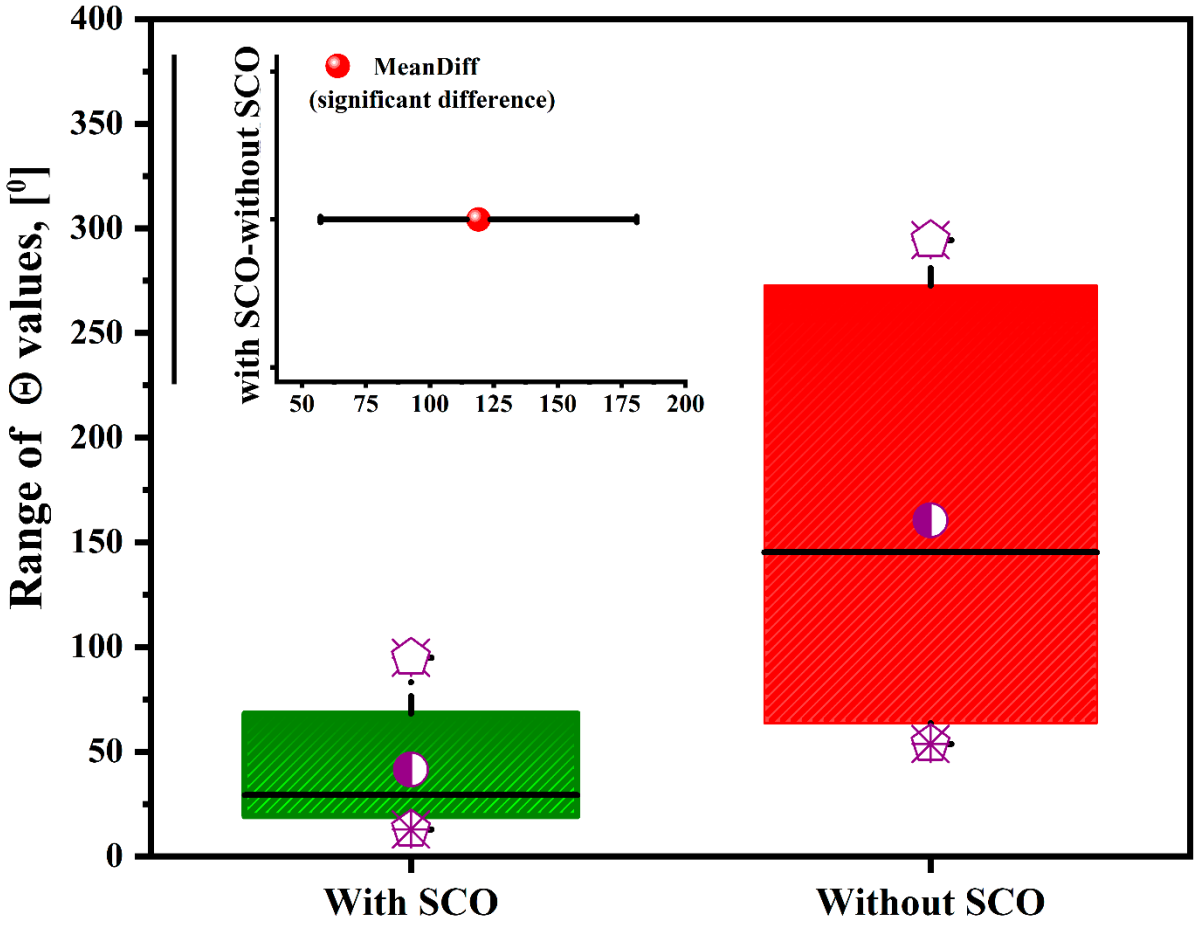

Figure S17. ANOVA analysis for the distortion index θ of the iron atom coordination polyhedron in $Fe(L)_2[M(CN)_4]$ Hofmann-like coordination polymers with and without SCO.

MS1: Additional details on the XPS data processing.

The recorded XPS spectra were compared with the ones obtained for the potassium salts to study the changes in electron density after the formation of the hybrid solids. For this reason, it is important to clarify that these comparisons were carried out through binding energies, and not through intensity. Regarding the relative peak area, it is important to note that the area under the curve of a photopeak in an XPS spectrum is related to the atomic concentration of each chemical species within the sample. In the compounds that were analyzed, their stoichiometry is known, which allows us to know the ratio between the populations of functional groups in the material. From this information, it is possible to establish the relationship of intensities of the different signals that make up the spectra fitting. However, it is important to consider that the C-C contribution is notably more intense due to the presence of adventitious contamination.

MS2: Computational Method and software package used.

Structure optimization for the high-temperature phases was performed with VASP (Viena Ab-Initio Simulation Package, version 5.4.4) software. DFT Spin-polarized calculations were carried out on the HS unit cell structure using the projected augmented-wave method (PAW) implemented in VASP. The general gradient approximated Perdew-Burke-Ernzerhof exchange-correlation density functional (GGA-PBE) was used considering its reported accuracy but above all for its efficiency in the prediction of the electronic structure and distance bonds. Spin-orbit coupling was incorporated to treat possible relativistic effects on the heavier atoms (Pd and Pt), likewise, scalar relativistic effects are included since the construction of PAW pseudopotentials. Van der Waals (vdW) dispersion corrections were incorporated according to the method of Grimme (DFT-D3), using the Becke-Jhonson damping function (BJ). The cutoff energy was optimized together with the k-points grid (Mokhorst-Pack) to 700 eV and 6×6×4, respectively. Full structural relaxation considered all the lattice parameters and the atomic positions. The force convergence threshold was set to values less than 0.02 eV/Å with an energy convergence value of 1×10^{-5} eV.

NBO charges computations were performed with Gaussian 09 software package at m062x/aug-cc-tzvp level of theory for the molecular segments constituted by the Fe-L in the vacuum. The

computations were performed in two steps: structural optimization and single point energy (NBO) calculations.

For the analysis of variance (ANOVA) the procedure implemented in the Origin data processing package was used

Table S1. Details of data collection, crystal data, and structure refinement for $Fe(3OHPy)_2[M(CN)_4]$ series with M = Ni, Pd and Pt at 300 K and 0K (calculated).

	$Fe(3OHPy)_2[Pt(CN)_4]$		**$Fe(3OHPy)_2[Pd(CN)_4]$**		**$Fe(3OHPy)_2[Ni(CN)_4]$**	
Data collection						
Diffractometer	D8 Advance (from Bruker)					
Detector	lynx eye					
Wavelength (Å)	CuK_a: 1.54183					
2θ range (°)	6.0-70.0		6.0-70.0		5.0-70.0	
Step size (°)	0.010591		0.010591		0.02044	
Time per step (s)	0.01		0.01		0.01	
Unit cell						
Space Group	C2/m		C2/m		C2/m	
Cell Parameters	a= 15.7130(7) Å		a= 15.7521(8) Å		a= 15.7988(2) Å	
	b= 7.4629(4) Å		b= 7.4646(4) Å		b= 7.2962(5) Å	
	c= 7.3933(4) Å		c= 7.4189(4) Å		c= 7.2162(5) Å	
	β= 99.33(2)º		β= 99.64(2)º		β= 101.11(2)º	
V(Å^3)	855.5(2)		860.0(2)		816.2(4)	
Z	2		2		2	
Refinement						
# of reflections	215				202	
# *of refined parameters*	Structural	Profile	Structural	Profile	Structural	Profile
	25	12	25	12	25	12
R_{exp}	2.83		2.82		2.84	
R_{wp}	8.15		8.14		7.83	
R_B	6.07		5.72		5.49	
S	2.87		2.88		2.75	
Calculated unit cell parameters for the low spin phases						
	$Fe(3OHPy)_2[Pt(CN)_4]$		$Fe(3OHPy)_2[Pd(CN)_4]$		$Fe(3OHPy)_2[Ni(CN)_4]$	
Space Group	C2/m		C2/m		C2/m	
Cell Parameter	a= 15.1911 Å		a= 15.6014 Å		a= 15.2890 Å	
	b= 7.0974 Å		b= 6.9847 Å		b= 6.8928 Å	
	c= 7.3830 Å		c= 7.4048 Å		c= 7.1237 Å	
	β= 99.61º		β= 98.38º		β= 99.10 º	
V(Å^3)	784.8		798.3		741.2	
Z	2		2		2	

Table S2. Results of elemental chemicals analysis for the $Fe(3OHPy)_2[M(CN)_4]$ series with M = Ni, Pd, Pt.

Metal	%Fe		%M		%C		%N		%O		%H	
	Cal.	Exp.	Cal.	Exp.	Cal.	Exp.	Cal.	Exp.	Cal.	Exp.	Cal.	Exp.
Ni	13.66	13.97	14.36	14.89	41.14	42.04	20.56	21.01	7.83	7.81	2.44	2.35
Pd	12.23	11.98	23.31	22.54	36.84	37.03	18.41	17.45	7.01	7.43	2.19	2.22
Pt	10.24	10.01	35.78	35.07	30.85	30.02	15.42	15.10	5.87	5.54	1.83	1.56

Table S3. Refined atomic positions and thermal (B_{iso}) and occupation (O_{cc}) factors for the materials under study.

Composition	site	x	y	z	Biso	Occ
$Fe(3\text{-}OHPy)_2[Pt(CN)_4]$						
Pt	2c	0	0	0.5	1.97(2)	1
Fe	2b	0	0.5	0	2.06(2)	1
C1	8j	0.0100(3)	0.1659(4)	0.3036(4)	3.1(3)	1
N1	8j	0.0054(3)	0.2710(3)	0.1953(3)	3.1(3)	1
N2	4i	0.1389(2)	0.5	0.0170(3)	3.1(3)	1
C2	4i	0.1652(4)	0.5	-0.1459(5)	3.1(3)	1
C3	4i	0.2508(4)	0.5	-0.1704(3)	3.1(3)	1
C4	4i	0.3134(3)	0.5	-0.0180(2)	3.1(3)	1
C5	4i	0.2888(2)	0.5	0.1519(4)	3.1(3)	1
C6	4i	0.2015(4)	0.5	0.1620(5)	3.1(3)	1
O	4i	0.2729(3)	0.5	-0.3377(4)	3.1(3)	1
$Fe(3\text{-}OHPy)_2[Pd(CN)_4]$						
Pd	2c	0	0	0.5	2.04(2)	1
Fe	2b	0	0.5	0	2.15(2)	1
C1	8j	0.0120(8)	0.1657(8)	0.3039(6)	3.3(3)	1
N1	8j	0.0057(7)	0.2713(6)	0.1958(5)	3.3(3)	1
N2	4i	0.1384(9)	0.5	0.0175(7)	3.3(3)	1
C2	4i	0.1653(6)	0.5	-0.1460(6)	3.3(3)	1
C3	4i	0.2509(4)	0.5	-0.1703(5)	3.3(3)	1
C4	4i	0.3138(6)	0.5	-0.0177(5)	3.3(3)	1
C5	4i	0.2882(4)	0.5	0.1512(7)	3.3(3)	1
C6	4i	0.2013(7)	0.5	0.1622(6)	3.3(3)	1
O	4i	0.2730(6)	0.5	-0.3376(5)	3.3(3)	1
$Fe(3\text{-}OHPy)_2[Ni(CN)_4]$						
Ni	2c	0	0	0.5	2.06(2)	1
Fe	2b	0	0.5	0	2.23(2)	1
C1	8j	0.0102(5)	0.1690(5)	0.2999(5)	3.4(3)	1
N1	8j	0.0052(4)	0.2749(4)	0.1913(4)	3.4(3)	1
N2	4i	0.1389(6)	0.5	0.0170(4)	3.4(3)	1
C2	4i	0.1652(5)	0.5	-0.1459(6)	3.4(3)	1
C3	4i	0.2508(6)	0.5	-0.1704(4)	3.4(3)	1
C4	4i	0.3134(6)	0.5	-0.0180(5)	3.4(3)	1
C5	4i	0.2888(5)	0.5	0.1519(6)	3.4(3)	1
C6	4i	0.2015(5)	0.5	0.1620(6)	3.4(3)	1

O	4i	0.2729(4)	0.5	-0.3377(5)	3.4(3)	1

Table S4. Calculated inter-atomic distances (in Å) and bond angles (in °), from the refined crystal structures, for the materials under study.

Bond distance (Å)	**Angles (°)**	
$Fe(3OHPy)_2[Pt(CN)_4]$		
Fe-N1 = 2.230(2)	N1-Fe-N2 = 91.73(2)	Fe-N2-C2 = 113.83(3)
Fe-N2 = 2.166(1)	N1-Fe-N2 = 88.27(2)	N2-C2-C3 = 124.52(4)
Pt-C1 = 1.934(2)	N1-Fe-N1 = 79.94(3)	C2-C3-C4 = 118.36(4)
C1-N1 = 1.115(1)	N1-Fe-N1 = 100.06(3)	C3-C4-C5 = 118.77(6)
N2-C2 = 1.335(2)	N2-Fe-N2 = 180.0	C4-C5-C6 = 118.51(4)
C2-C3 = 1.386(1)	C1-Pt-C1 = 79.61(3)	C5-C6-N2 = 124.39(4)
C3-C4 = 1.370(1)	C1-Pt-C1 = 100.39(4)	C6-N2-Fe = 130.72(3)
C4-C5 = 1.373(2)	N1-C1-Pt = 170.407(6)	C6-N2-C2 = 115.45(6)
C5-C6 = 1.386(1)	C1-N1-Fe = 174.547(5)	C2-C3-O = 121.58(4)
C6-N2 = 1.332(1)		C4-C3-O = 120.06(6)
C3-O = 1.338(2)		
$Fe(3OHPy)_2[Pd(CN)_4]$		
Fe-N1 = 2.234(2)	N1-Fe-N2 = 91.76(2)	Fe-N2-C2 = 114.27(3)
Fe-N2 = 2.162(1)	N1-Fe-N2 = 88.24(2)	N2-C2-C3 = 125.01(4)
Pd-C1 = 1.943(2)	N1-Fe-N1 = 80.31(3)	C2-C3-C4 = 118.33(4)
C1-N1 = 1.117(1)	N1-Fe-N1 = 99.69(3)	C3-C4-C5 = 117.93(6)
N2-C2 = 1.350(2)	N2-Fe-N2 = 180.0	C4-C5-C6 = 119.73(4)
C2-C3 = 1.390(1)	C1-Pd-C1 = 79.09(3)	C5-C6-N2 = 124.13(4)
C3-C4 = 1.374(1)	C1-Pd-C1 = 100.91(4)	C6-N2-Fe = 130.86(3)
C4-C5 = 1.379(2)	N1-C1-Pd = 168.20(5)	C6-N2-C2 = 114.87(6)
C5-C6 = 1.385(1)	C1-N1-Fe = 174.48(5)	C2-C3-O = 121.78(4)
C6-N2 = 1.333(1)		C4-C3-O = 119.89(6)
C3-O = 1.344(2)		
$Fe(3\text{-}OHPy)_2[Ni(CN)_4]$		
Fe-N1 = 2.137(2)	N1-Fe-N2 = 92.91(2)	Fe-N2-C2 = 115.92(3)
Fe-N2 = 2.174(1)	N1-Fe-N2 = 87.09(2)	N2-C2-C3 = 126.23(4)
Ni-C1 = 1.929(2)	N1-Fe-N1 = 79.54(3)	C2-C3-C4 = 118.63(4)
C1-N1 = 1.092(1)	N1-Fe-N1 = 100.46(3)	C3-C4-C5 = 116.79(6)
N2-C2 = 1.320(2)	N2-Fe-N2 = 180.0	C4-C5-C6 = 120.38(4)
C2-C3 = 1.397(1)	C1-Ni-C1 = 79.47(3)	C5-C6-N2 = 124.55(4)
C3-C4 = 1.330(1)	C1-Ni-C1 = 100.53(4)	C6-N2-Fe = 130.66(3)
C4-C5 = 1.356(2)	N1-C1-Ni = 169.77(6)	C6-N2-C2 = 113.42(6)
C5-C6 = 1.395(1)	C1-N1-Fe = 174.54(5)	C2-C3-O = 123.28(4)
C6-N2 = 1.294(1)		C4-C3-O = 118.09(6)
C3-O = 1.320(2)		

Table S5. Details of the crystal data for six Hofmann-like coordination polymers without spin crossover. These six compositions were prepared and their crystal structure solved and refined.

M	Ligand	SG	Cell parameters	Cell volume	Ref. (CCDC)*
4-Ethynylpyridine (Ni) $Fe(C_7N)_2[Ni(CN)_4]$	4EPy	I2/m	a=18.3802 Å b=7.4668 Å c=6.8675 Å β=96.0170°	V=937.31 Å^3	2251855
4-Iodopyridine (Ni) $Fe(C_5NI)_2[Ni(CN)_4]$	4IPy	I2/m	a=18.3630 Å b=7.4646 Å c=6.7483 Å β=95.2197°	V=921.17 Å^3	2251856
4-Hydroxypyridine (Ni) $Fe(C_5NO)_2[Ni(CN)_4]$	4OHPy	$P2_1$	a=10.3432 Å b=10.2877 Å c=7.7411 Å β=101.8650°	V=806.11 Å^3	2251857
5-Ethynylpyrimidine (Ni) $Fe(C_6N_2)_2[Ni(CN)_4]$	5EPym	$P2_1$	a=16.3432 Å b=6.9451 Å c=7.6366 Å β=91.5604°	V=866.47 Å^3	2251858
Ethyl Nicotinate (Ni) $Fe(C_8NO_2)_2[Ni(CN)_4]$	ENicotinate	$Pmn2_1$	a=7.3773 Å b=6.8461 Å c=23.4674 Å	V=1185.24 Å^3	2251859
1-Vinyl-1,2,4-triazole (Ni) $Fe(C_4N_3)_2[Ni(CN)_4]$	VTzole	Pnma	a=13.2282 Å b=7.2625 Å c=16.9247 Å	V=1625.96 Å^3	2251860

*) Numbers for the CIF files deposited in the CCDC database.

Table S6. Distortion indexes Σ, Θ, and CShM for the iron atom coordination environment in the $Fe(L)_2[Ni(CN)_4]$ solids formed using different organic molecules (L) as axial ligands. Pillared solids with and without SCO were considered.

M	SCO ?	Σ	Θ	CShM	Reference
1-Vinyl-1,2,4-triazole (Ni)	No	147.325	145.345	2.6292	This work (Table S5)
4-Iodopyridine (Ni)	No	165.762	269.293	4.1787	This work (Table S5)
4-Ethynylpyridine (Ni)	No	168.145	276.087	4.4131	This work (Table S5)
4-Hydroxypyridine (Ni)	No	55.106	78.725	0.6698	This work (Table S5)
5-Ethynylpyrimidine (Ni)	No	129.092	199.932	2.8544	This work (Table S5)
Ethyl Nicotinate (Ni)	No	168.45	294.406	5.5558	This work (Table S5)
4-Phenylpyridine (Pt)	Yes	9.804	18.966	0.0354	[c]
4,4-Bipyridine (Ni)	Yes	16.529	19.812	0.0629	[d]
Pyrazine (Pt)	Yes	0	25.000	0.0496	[e]
2-Ethylimidazole (Ni)	No	70.268	95.731	0.6690	[f]
2-Methylimidazole (Ni)	No	22.724	67.506	0.1248	
Benzimidazole (Ni)	No	46.506	80.741	0.6528	
2-Imidazole (Ni)	No	50.288	60.554	0.2754	[g]
Thiazole (Ni)	No	30.556	44.088	0.1280	[h]
3-Aminopyridine (Ni)	Yes	13.82	19.396	0.0313	[i]
3-Methylpyridine (Ni)	Yes	0.076	34.556	0.091	[j]
4-Methylpyrdine (Ni)	No	69.280	53.924	0.256	
2,4 Bipyridine (Pt)	Yes	16.529	19.812	0.0629	[k]
bis(4-pyridyl)acetylene) (Ni)	Yes	0	16.608	0.0219	[l]

CShM: continuous shape measure was calculated using CoSyM-Continuous Symmetry Measures https://csm.ouproj.org.il/; References [c]: Spectroscopic, Structural, and Magnetic Studies. Inorganic chemistry, 48(13), 6130-6141; [d]: Magnetochemistry, 2(1), 8; [e]: Journal of the American Chemical Society, 130(28), 9019-9024; [f]: Journal of Solid State Chemistry, 204, 128-135; [g]: Journal of Solid State Chemistry, 197, 317-322; [h]: Polyhedron, 95, 75-80; [i]: Inorganic Chemistry, 54(17), 8711-8716; [j]: Molecular Crystals and Liquid Crystals Science and Technology. Section A. Molecular Crystals and Liquid Crystals, 341(2), 527-532; [k]: Inorganic Chemistry, 60(16), 11866-11877; [l]: Chemistry–A European Journal, 18(2), 507-516.

Table S7. Relevant interatomic distances (in Å), and calculated distortion indexes Σ, Θ, and CShM for the iron atom coordination polyhedron in the high spin phases in the $Fe(3XPy)_2[M(CN)_4]$ series with X = F, Cl, Br, and I.

X	Phase	SCO ?	Fe– N_{Py}	Fe–N_{CN}	Σ	Θ	CShM	Ref.
Py	HS (295 K), XRD	Yes	2.28(95)	2.13(63)	16.80	37.26	0.1305	[a]
3FPy	HS (295 K), XRD	Yes	2.00(47)	2.09(18)	32.89	45.40	0.1985	[a]
3ClPy	HS (295 K), XRD	Yes	2.18(11)	2.09(24)	17.27	29.26	0.1094	[a]
3BrPy	HS (295 K), XRD	No	2.23(11)	2.12(53)	37.23	53.69	0.2357	[a]
3ICl	HS (295 K), XRD	No	2.08(80)	2.15(65)	54.90	73.42	0.35	[a]

CShM: continuous shape measure was calculated using CoSyM-Continuous Symmetry Measures https://csm.ouproj.org.il/; Reference [a]: J. Solid State Chem., 2020, 282, 121070

Table S8. Relevant interatomic distances (in Å), and distortion indexes Σ, Θ, and CShM for the for the iron atom coordination polyhedron in $Fe(3EPy)_2[M(CN)_4]$ series with M=Ni, Pd and Pt; (3EPy = 3Ethynylpyridine)

M	Phase	SCO ?	Fe– N_{Py}	Fe–N_{CN}	Σ	Θ	CShM	Ref.
Ni	HS (295 K), XRD LS calculated	Yes	2.25(14) 2.00(1186)	2.31 (6) 1.99(404)	26.35 22.71	51.95 44.59	0.3453 0.1816	[b]
Pd	HS (295 K), XRD LS calculated	Yes	2.20(7) 2.00(1148)	2.21(6) 2.02(388)	59.68 45.35	109.78 75.49	0.9893 0.4283	[b]
Pt	HS (295 K), XRD LS calculated	Yes	2.20(13) 1.99(1164)	2.18(15) 1.96(518)	46.25 26.98	90.33 56.14	0.7527 0.2517	[b]

CShM: continuous shape measure was calculated using CoSyM-Continuous Symmetry Measures https://csm.ouproj.org.il/; Reference [b]: *New J. Chem*. 2022, 46, 9618-9628

Table S9. Calculated electron density at the N-pyridinic atom, according to NBO, for different pyridine derivatives as pillar molecules. The NBO analysis was applied in the structures previously optimized (relaxed) according to the method described in the computational methods section.

Ligand	Electron density at the pyridinic N atom	SCO ?	Reference
1,2-di(4-Pyridyl)ethylene	-0.511	Yes	This work
1,4-bis(4-pyridylethynyl)benzene	-0.48	Yes	"
2-Methylpyrdine	-0.5	Yes	"
3-Methylpyrdine	-0.508	Yes	"
3-Fluoropyrazine	-0.51	Yes	"
3-Fluoropyridine	-0.493	Yes	"
3-Chloropyridine	-0.495	Yes	"
3-Bromopyridine	-0.523	Yes	"
3-Iodopyridine	-0.532	Yes	"
3-Ethynylpyridine	-0.473	Yes	"
3-Hydroxipyridine	-0.504	Yes	"
3-Aminopyridine	-0.515	Yes	"
4-Fluoropyridine	-0.51	Yes	"
4-Chloropyridine	-0.507	Yes	"
4-Bromopyridine	-0.526	Yes	"
4-Iodopyridine	-0.529	Yes	"
4,4-Bipyridine	-0.507	Yes	"
4,4-Azopyridine	-0.496	Yes	"
Imidazol[1,2-a]Pyridine	-0.586	No	"
Pyrazine	-0.452	Yes	"
Pyridine	-0.481	Yes	"
2-Ethynylpyridine	-0.479	No	"
4-(2-Pyridin-4-ylethyl)Pyridine	-0.577	No	"
4-Acetylpyridine	-0.486	No	"
4-Methylpyrdine	-0.521	No	"
4-Pyridine Carboxyaldehyde	-0.463	No	"
4-Vynylpyridine	-0.514	No	"
Nicotinamide	-0.516	No	"
Nicotinic acid	-0.52	No	"

Table S10. Calculated electron density at the N-pyridinic atom, according to NBO, for thiazole, oxazole, and imidazole and its derivatives. The NBO analysis was applied in the structures previously optimized (relaxed) according to the method described in the computational methods section.

Ligand	Electron density at the pyridinic N atom	SCO ?	Reference
Imidazole	-0.560	No	This work
2-methyl imidazole	-0.563	No	"
2-ethyl imidazole	-0.562	No	"
Benzimidazole	-0.556	No	"
Thiazole	-0.512	No	"
Oxazole	-0.598	No	"

Table S11. Values of N_{1s} core-level binding energy (BE) of the pyridinic N atom, from XPS measurements, for the $Fe(L)_2[Ni(CN)_4]$ solids obtained with different organic molecules as axial ligands (L). Pillared solids with and without SCO were considered.

With SCO		
Ligand and inner metal (M)	**N1s, in eV**	
	CN	**C-N=C**
3-Hidroxypyridine (Ni)	398.58	399.43
3-Hidroxypyridine (Pd)	398.63	399.39
3-Hidroxypyridine (Pt)	398.64	399.38
3-Fluoropyridine (Ni)	398.6	399.76
3-Ethynilpyridine (Pd)	398.6	399.52
3-Ethynilpyridine (Pt)	398.53	399.57
3-Aminopyridine (Ni)	398.59	399.35
3-Methylpyridine (Ni)	398.52	399.4
4,4-Bipyridine (Ni)	398.15	399.03
4-Phenylpyridine (Ni)	398.49	399.35
Without SCO		
Ligand and inner metal (M)	**N1s, in eV**	
	CN	**C-N=C**
2-Pyridineethanol (Ni)	398.46	399.3
2-Vinyl pyrazine (Ni)	398.41	399.66
3-Bromopyridine (Ni)	398.49	399.59
3-Iodopyridine (Ni)	398.5	399.59
4-Ethylpyridine (Ni)	398.44	399.35

4-ChloroPyridine (Ni)	398.5	399.47
4-Iodopyridine (Ni)	398.51	399.49
4-Hydroxypyridine (Ni)	398.55	400.07
5-Ethynilpyrimidine (Ni)	398.55	399.72
nicotinic Acid (Ni)	398.37	400.08
Imidazole (Ni)	398.62	400.46
2-methyl imidazole (Ni)	398.66	400.39
2-ethyl imidazole (Ni)	398.68	400.37
Benzimidazole (Ni)	398.96	400.78
Thiazole (Ni)	398.49	399.39

Source of the data reported in this Table: This work

Table S12. Frequency, in cm^{-1}, of the ν(CN) band values from IR spectra for the $Fe(L)_2[Ni(CN)_4]$ solids formed using different organic molecules (L) as axial ligands. Pillared solids with and without SCO were considered.

With SCO		**Without SCO**	
Ligand and inner metal (M)	**ν(CN)**	**Ligand and inner metal (M)**	**ν(CN)**
3-Fluoropyridine (Ni)	2161	1-Vinyl-1,2,4-triazole (Ni)	2147
3-Chloropyridine (Ni)	2156	2-Vinyl pyrazine (Ni)	2146
3-Methylpyridine (Ni)	2155	3-Bromopyridine (Ni)	2149
3-Ethynylpyridine (Ni)	2155	3-Iodopyridine (Ni)	2150
3-Hidroxypyridine (Ni)	2159	4-Chloropyridine (Ni)	2148
3-Aminopyridine (Ni)	2155	4-Bromopyridine (Ni)	2150
4,4-Bipyridine (Ni)	2151	4-Iodopyridine (Ni)	2150
4-Phenylpyridine (Ni)	2152	4-Ethylpyridine (Ni)	2148
bis(4-pyridyl)butadiyne (Ni)	2154	Ethyl Nicotinate (Ni)	2149
Ethane (Ni)	2151	Methyl Nicotinate (Ni)	2150
Ethylene (Ni)	2160	Nicotinamide (Ni)	2149
Pyrazine (Ni)	2153	Nicotinic Acid (Ni)	2146
Pyridine (Ni)	2158	Imidazo[1,2-A]pyridine (Ni)	2149
Pyridazine (Ni)	2159	Imidazo[1,2-A]pyrazine (Ni)	2150

Source of the data reported in this Table: This work

Table S13. Frequency, in cm^{-1}, obtained for the Fe-N_L, from the calculated Raman spectra, for the $Fe(L)_2[Ni(CN)_4]$ solids formed using different organic molecules (L) as axial ligands. Pillared solids with and without SCO were considered.

With SCO		**Without SCO**	
	ν(Fe-N_L)		**ν(Fe-N_L)**
Pyridine (Ni)	240	1-Vinyl-1,2,4-triazole (Ni)	286
2-Chloropyrazine (Ni)	289	2-PyridineEthanol (Ni)	275
3-Fluoropyridine (Ni)	284	3-Bromopyridine (Ni)	265
3-Chloropyridine (Ni)	274	3-(2-Hydroxyethyl) pyridine (Ni)	278
3-Methylpyridine (Ni)	281	4-Methylpyridine (Ni)	270
3-Hidroxypyridine (Ni)	283	4-Ethylpyridine (Ni)	263
3-Ethynylpyridine (Ni)	282	4-Hydroxypyridine (Ni)	272
3-Aminopyridine (Ni)	284	5-Ethynilpyridine (Ni)	275
4,4-Bipyridine (Ni)	290	Methyl Nicotinate (Ni)	274
bis(4-pyridyl)butadiyne (Ni)	301	Ethyl Nicotinate (Ni)	271
4-Benzylpyridine (Ni)	242	Nicotinamide (Ni)	274
Pyrazine (Ni)	301	Nicotinic Acid (Ni)	276
Pyridazine (Ni)	306		

Source of the data reported in this Table: This work

Table S14. Mössbauer parameter Δ_{QS}, at room temperature, for a group of ferrous tetracyanometallates with and without spin crossover.

Label, in Fig.10D	Material	SCO?	Δ_{QS}, mm/s	Reference
1	FePyNPTCN	Yes	0.86	T. Kitazawa, K. Hosoya, M. Takahashi, M. Takeda, I. Marchuk, S. M. Filipek, *J. Radioanal. Nucl. Chem.*, 2003, *255*, 509-512.
2	Fe3ClPyTCN	Yes	1.3	T. Kitazawa, M. Takahashi, M. Takahashi, M. Enomoto, A. Miyazaki, T. Enoki, M. Takeda, *J. Radioanal. Nucl. Chem.*, 1999, *239*, 285-290.
3	FeAzpyNi	Yes	1.16	I. Boldog, A. G. Gaspar, V. Martínez, P. Pardo-Ibañez, V. Ksenofontov, A. Bhattacharjee, ….., J. A. Real. *Angew. Chemie*, 2008, *120*, 6533-6537.
4	FeAzpyPt	Yes	0.85	
5	FeAzpyPd	Yes	0.83	
6	FeAzpyPt•H_2O	Yes	0.86	
7	FeAzpyPd•nH_2O	Yes	0.89	
8	FeNH_2PyNi	Yes	0.92	W. Liu, L. Wang, Y. J. Su, Y. C. Chen, J. Tucek, R. Zboril, ... & M. L. Tong. *Inorg. Chem.*, 2015, *54*, 8711-8716.
9	FeNH_2PyPt	Yes	0.74	
10	FebpacPt•H_2O•0.71bpac	Yes	0.82	C. Bartual-Murgui, L. Salmon, A. Akou, N. A. Ortega-Villar, H. J. Shepherd, M. C. Muñoz, A. Bousseksou, *Chem.–A Europ. J.*, 2012, *18*, 507-516.
11	Fe3OHPyNi	Yes	1.33	This work
12	Fe3OHPyPd	Yes	1.31	
13	Fe3OHPyPt	Yes	1.31	
14	Fe3ClPyTCN	No	2.68	T. Kitazawa, M. Takahashi, M. Takahashi, M. Enomoto, A. Miyazaki, T. Enoki, M. Takeda. *J. Radioanal. Nucl. Chem.* 1999, *239*, 285-290.
15	FePyzPtH•H_2O	No	2.86	G. Agusti, S. Cobo, A. B. Gaspar, G. Molnar, N. O. Moussa, P. A. Szilagyi, P. A., ...A. Bousseksou, A. *Chem. Mater.*, 2008, *20,* 6721-6732.
16	FePyzPt•2.5H_2O	No	2.77	
17	FeAzpyPd•nH_2O	No	2.93	
18	FeAzpyPt•nH_2O	No	2.9	
19	FeAzpyPd	No	2.3	
20	FebpacPt•H_2O•0.09bpac	No	2.75	C. Bartual-Murgui, L. Salmon, A. Akou, N. A. Ortega-Villar, H. J. Shepherd, M. C. Muñoz, ... & A. Bousseksou, *Chemistry–A European Journal*, 2012, *18*, 507-516.

CCDC Numbers for the six additional crystal structures solved and refined for Hofmann-like coordination polymers without SCO used to calculate the distortion indexes for the iron coordination polyhedron.

Deposition Number 2251855
Compound Name: 4-Ethynylpyridine
Data Block Name: data_Fe(4-Ethynylpyridine)2[Ni(CN)4]
Unit Cell Parameters: a 18.3802(2) b 7.4667(2) c 6.8675(3) I2/m
---
Deposition Number 2251856
Compound Name:4-Iodopyridine
Data Block Name: data_Fe(4-Iodopyridine)2[Ni(CN)4]
Unit Cell Parameters: a 18.3630(2) b 7.4646(2) c 6.7483(3) I2/m
---
Deposition Number 2251857
Compound Name: 4-Hydroxypyridine
Data Block Name: data_Fe(4-Hydroxypyridine)2[Ni(CN)4]
Unit Cell Parameters: a 10.3432(2) b 10.2877(2) c 7.7411(3) P21

Deposition Number 2251858
Compound Name: 5-Ethynylpyrimidine
Data Block Name: data_Fe(5-Ethynylpyrimidine)2[Ni(CN)4]
Unit Cell Parameters: a 16.3432(2) b 6.9451(2) c 7.6366(3) P21

Deposition Number 2251859
Compound Name: Ethyl-Nicotinate
Data Block Name: data_Fe(Ethyl-Nicotinate)2[Ni(CN)4]
Unit Cell Parameters: a 7.3773(2) b 6.8461(3) c 23.4674(2) Pmn21

Deposition Number 2251860
Compound Name: Vinyl-triazole
Data Block Name: data_Fe(Vinyl-triazole)2[Ni(CN)4]
Unit Cell Parameters: a 13.2282(3) b 7.2625(2) c 16.9247(3) Pnma